Radio frequency–infrared doubleresonance and multiphoton Lamb dips in a dressed molecule

E. Arimondo, A. Sasso, and M. Allegrini

Citation: The Journal of Chemical Physics **84**, 2439 (1986); doi: 10.1063/1.450362
View online: http://dx.doi.org/10.1063/1.450362
View Table of Contents: http://scitation.aip.org/content/aip/journal/jcp/84/5?ver=pdfcov
Published by the AIP Publishing

Radio frequency–infrared double-resonance and multiphoton Lamb dips in a dressed molecule

E. Arimondo and A. Sasso
Istituto di Fisica Sperimentale, Universitá di Napoli, Pad. 20 Mostra d'Oltremare, 80125 Napoli, Italy
M. Allegrini
Istituto di Fisica Atomica e Molecolare del C.N.R., Via del Giardino 7, 56100 Pisa, Italy

(Received 21 June 1985; accepted 15 October 1985)

The molecular response in laser intracavity experiments where molecules interact simultaneously with a radio frequency field and an infrared one is analyzed theoretically. In the quantized field approach the molecule–radio frequency interaction is treated exactly. For the laser intensity the density matrix equations are solved either in a third-order perturbation treatment or through a matrix continued fraction analysis. The resonance line shapes in different two-level and three-level configurations are analyzed numerically.

I. INTRODUCTION

In infrared–radio frequency double-resonance experiments a molecular gas is submitted to the simultaneous action of a radio frequency (or microwave) radiation and an infrared laser beam. The absorption of the radio frequency (rf) field is detected as a power variation of the infrared (IR) beam propagating through the sample.[1] Typically, in the double-resonance experiments a high sensitivity is achieved because the absorption of rf photons is detected as a change in the number of IR photons reaching the detector, and because the thermal distribution of population over the levels of the rf transition is modified by the laser radiation. In experiments inside the laser cavity, where the variation in the laser output power is detected, the sensitivity is enhanced by the nonlinear operation of the laser near threshold.[2,3] Moreover the linewidth of the double-resonance signals is broadened by the laser pumping action and the line shape depends on the laser intensity for strong laser radiation or for IR transitions with large transition dipole moment.[4–8] In the intracavity experiments where a standing-wave laser radiation interacts with the sample, inverted Lamb dips appear on the laser output power whenever the laser frequency matches a transition of the absorbing medium. The infrared transition frequencies are determined with a very high accuracy by measuring the position of the inverted Lamb dip. If the absorption frequencies are outside the tunability of the laser, a radio frequency (or microwave) field can be applied to the sample and multiphoton Lamb dips may occur. These dips were first observed by Freund and Oka[9] in infrared–microwave experiments in ammonia and have been later used for high-resolution molecular spectroscopy.[10] Sub-Doppler resonances occur also when the two running waves of a laser field are in resonance with transitions sharing a common level (cross-saturation resonances) or when the absorption of several infrared photons is involved (velocity-tuned multiphoton Lamb dips).[11]

The sub-Doppler resonances present different features depending on the level configuration involved in the IR–rf absorption. For molecules with a permanent dipole moment, each level is split into sideband levels separated by the rf photon energy. An IR absorption occurs whenever the IR laser is in resonance with the splitting between two sideband levels. In the double-resonance configuration the rf field is in resonance with a two-level transition, and an infrared laser transition from any one of these levels to a third level is perturbed by the rf absorption.

Several theoretical approaches have been used to interpret the resonance positions and the line shape of the IR–rf experiments where there is a resonant interaction of two radiation fields with a three-level system. For the case of a running wave laser and for a set of molecules (or atoms) with a given velocity the density matrix equations have been solved analytically by Brewer and Hahn[12] in a Bloch-like form. This solution is very convenient for interpreting the saturation phenomena produced by strong IR laser and rf radiation. In the rate-equation approximation, where the coherences created by the two-photon absorption processes are neglected, an integration over the Boltzmann velocity distribution of the absorbing molecules has been performed by Wormsbecher *et al.*[13] The density matrix solution of Ref. 12 has been numerically integrated over the Boltzmann distribution by Takami[14] in order to describe the results of optical-microwave double-resonance experiments. The case of standing-wave laser radiation has been considered by Oka[2] in the rate-equation approximation. The IR–rf multiphoton Lamb dips have been described theoretically by Shimizu[15] with a perturbation treatment based on a series expansion of the density matrix elements as function of both the IR and rf electric field intensities. Terms up to the seventh order in the electric fields were considered in the expansion and a continued fraction solution was sketched out to deal with very strong electric fields.

The dressed-atom approach is a formalism where rf field quantized states can be introduced and the rf interaction can be treated exactly. The density matrix equations are solved for the interaction with the IR laser field only. This method has been applied to treat the radio frequency interaction in intracavity experiments, mainly for the two-level multiphoton Lamb dips.[2,8,10,16] However, a complete treatment of the rf interaction in the laser intracavity experiments has never been presented, and several important configurations of the rf interaction have not been considered. For instance, the

 0021-9606/86/052439-12$02.10

double resonance, the multiphoton Lamb dips in three-level systems, and their simultaneous contribution to the observed signal have not been analyzed. We believe that the dressed-atom approach is the most convenient to investigate the three-level configuration. In this work the dressed-atom approach will be presented in detail and applied to the two most important level configurations: a two-level system with double-parity levels, for which the rf interaction depends on the permanent dipole moment, and the three-level system where the rf field induces transitions between two levels of the system. Following this discussion the line shapes of the double resonance and of the Doppler-free saturation resonances will be derived.

In the analysis of saturated absorption phenomena a standard approach for dealing with the laser interaction is to find the solution of the density-matrix equations at the third-order perturbation in the laser electric field amplitude. When the third-order solution is applied to a molecular system dressed by the rf field, the IR–rf multiphoton Lamb dips and the double resonance are simultaneously obtained. In fact, the Doppler integration of the third-order solution singles out the contributions of a molecular velocity group: both Lamb dips and double resonance involve the interaction of molecules in a given velocity group with saturating and probing IR running waves of the laser. For the Lamb dips these running waves are the counterpropagating components of a standing wave; for the double resonance the saturation and probe actions involve the same running wave. The third-order solution of the rf dressed molecule, previously applied to the two-level multiphoton Lamb dips,[2,10,11] is here reported for the three-level system.

The third-order perturbation solution cannot be applied in the strong IR field regime, where velocity tuned IR multiphoton processes occur. In this regime the solution of the density matrix equations must include all orders of expansion in the IR electric field intensity. It has been shown that for a three-level system interacting with standing-wave lasers the density matrix equations are conveniently solved through a matrix continued fraction.[17] With the dressed-atom approach applied to the double resonance we will obtain density matrix equations describing a three-level system interacting with two standing wave laser modes having the same frequency. The frequency and the intensity of the rf field determine the relative intensity of the laser modes. This configuration is solved through continued fractions of 4×4 matrices. A numerical analysis will be worked out to derive the line shapes of double resonance and Lamb dips. An increase in the IR electric field intensity requires calculation of the continued fraction with higher order terms.

This work mainly concerns the three-level IR–rf phenomena; the two-level dressed molecule description is briefly considered for completeness of the treatment only. The theoretical framework and the dressed atom formalism will be presented in Sec. II. The third-order solution for the IR field interaction and the integration over the velocity distribution is analyzed in Sec. III; a numerical analysis of the double-resonance line shape derived in third order has been reported in Ref. 18. The analysis of the IR–rf Doppler-free saturation resonances is presented in Sec. IV. The interaction with a strong standing wave laser radiation is treated in Sec. V.

In the intracavity experiments the sample polarizability at the IR frequency interacts with the IR laser field and both the real and imaginary parts of the polarizability, i.e., the refractive index and the absorption coefficient, determine the laser operation. The laser output power is then a unique function of the absorption coefficient only when the resonant frequency of the laser cavity is equal to that of the active medium as well as of the absorbing molecular medium. This coincidence of the resonant frequencies is seldom the case in actual experiments. In double-resonance experiments with laser frequency very far from the molecular absorption frequency, the so-called off-resonance experiments,[19] the influence of the refractive index was directly pointed out. In Ref. 15 the influence of the refractive index on the IR laser output power in double-resonance experiments was determined through a simple model for the laser oscillation conditions. A detailed description of the laser operation taking into account the refractive index and absorption coefficient and a comparison with the observed experimental features may require an enormous amount of numerical calculation. Thus, in the numerical calculations of this paper, based either on the third-order approximation or on the continued fraction, only the IR molecular absorption coefficient, i.e., the imaginary part of the molecular susceptibility, will be evaluated.

II. MOLECULES AND ELECTROMAGNETIC FIELDS

The molecular system is described by the wave functions $|\alpha\rangle$, $(\alpha = 1,2,...)$, eigenstates of the molecular Hamiltonian H_m with eigenvalues E_α,

$$H_m|\alpha\rangle = E_\alpha|\alpha\rangle. \tag{1}$$

As done previously by Shimizu,[15] our analysis will be restricted to the level configurations of Fig. 1 representing typical level schemes. In the two-level scheme of Fig. 1(a) the transition between levels $|1\rangle$ and $|2\rangle$, a vibrational IR transition, has a separation $\hbar\Omega_0$. The levels $|1\rangle$ and $|2\rangle$ are supposed to have permanent dipole moments μ_1 and μ_2, respectively, as for instance double parity levels in symmetric top molecules. In the three-level scheme of Fig. 1(b) the $\hbar\Omega_0$ transition $|1\rangle$–$|2\rangle$ is in the IR region. The $\hbar\omega_0$ transition between the levels $|2\rangle$ and $|3\rangle$, is a hyperfine or rotational transition in an excited vibrational state. The levels are supposed to have zero permanent dipole moments, but the

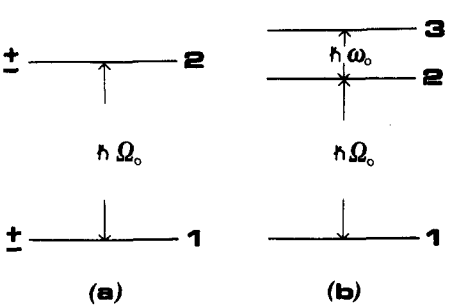

FIG. 1. Energy level schemes considered in this paper. Two-level system with double-parity levels (a) and three-level system with single-parity levels and a radio frequency (or microwave) splitting in the upper state (b).

transition between $|2\rangle$ and $|3\rangle$ levels may be induced by a radio frequency or microwave field. Such a configuration occurs for instance in the NH_3 molecule where the symmetric top levels are split by the inversion operation. Although the level scheme of Fig. 1(b) does not represent the most general three-level configuration, the solution for this configuration can be adopted for all other three-level schemes by changing the sign of ω_0 and Ω_0.[17,20] An important case not included in Fig. 1 because of mathematical complexity is a three-level scheme with double-parity levels, where all the three levels have permanent dipole moments.

The IR electric field of frequency Ω is assumed to have a $\cos kz$ plane-wave standing field distribution along the z axis of the optical cavity (see Fig. 2). The electric field interaction is described by the matrix elements μ_v for the vibrational electric dipole transition moment between the $|1\rangle$ and $|2\rangle$ states. The IR interaction Hamiltonian V^{IR} is described by the following matrix elements

$$V_{21}^{IR}(z,t) = V_{12}^{IR}(z,t) = -\mu_v E \cos \Omega t \cos kz. \tag{2}$$

The rf and IR interactions are treated through the standard approach of the laser theory for the ensemble-averaged molecular density matrix $\rho^m(v,z,t)$ of the molecules with velocity v along the z axis at position z and at time t.[21] The time evolution of the density matrix produced by the relaxation processes is described by

$$\frac{d}{dt}\rho^m = -\gamma[\rho^m - \Lambda^m(v)]. \tag{3}$$

As typical of IR–rf molecular systems a single relaxation rate has been introduced. The diagonal matrix $\Lambda^m(v)$ describes the uniform and constant population of the molecular levels at thermal equilibrium.

In a rf double-resonance experiment the equilibrium population difference between the levels $|2\rangle$ and $|3\rangle$ in resonance with the rf radiation is very small. Thus the signal intensity depends upon the pumping action of the IR radiation only. By contrast, in a microwave double-resonance experiment the thermal equilibrium population difference contributes to the signal. The most general treatment of double-resonance experiments inside a laser cavity should consider the population distribution over the levels of Fig. 1(b). However, we will consider only rf experiments, where the thermal population difference between the rf levels may be neglected. Thus, Eq. (3) will be solved supposing that at thermal equilibrium only the population for the lower $|1\rangle$ level is different from zero. The Maxwell–Boltzmann velocity distribution $W(v)$ for the velocity v along the z axis is introduced in the thermal population, and the pumping term

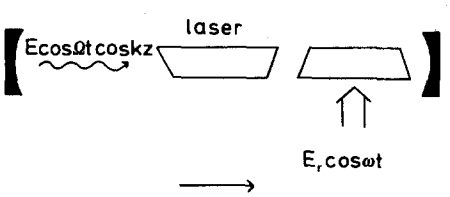

FIG. 2. Schematic of the experimental setup used in the intracavity investigations.

for the lower $|1\rangle$ level will be written as

$$\Lambda^1(v) = \Lambda^1 W(v) = (\sqrt{\pi}u)^{-1} \exp[-(v/u)^2], \tag{4}$$

where u denotes the most probable velocity.

The complex polarization of the molecular system is given by

$$P(z,t) = \mu_v \int_{-\infty}^{\infty} dv\, \rho_{12}^m(v,z,t) + \text{c.c.} \tag{5}$$

and the operation of the laser shown in Fig. 2 is affected by the Fourier component oscillating at frequency Ω with the spatial dependence $\cos kz$ of the IR field.[21] Thus, we define the bulk susceptibility χ of the intracavity absorber averaged over the unit length

$$\chi = \left[2 \int dz \cos kz P(z,t)\Big|_{+\Omega}\right][E \exp(+i\Omega t)]^{-1}, \tag{6}$$

where the term oscillating at frequency $+\Omega$ must be singled out in the molecular polarization.

In the dressed-atom picture[22–24] the rf field $E_r \cos \omega t$ is described by a harmonic oscillator at frequency ω with Hamiltonian

$$H_{rf} = \hbar\omega a^+ a, \tag{7}$$

where a and a^+ are the creation and annihilation operators for the rf photons. The eigenstates $|n\rangle$ involving n rf photons have energy $(n + 1/2)\hbar\omega$. The electric and magnetic fields are written as a function of the a and a^+ operators. The rf field in the absence of interactions with the molecules is represented by a coherent state

$$|\psi_{rf}(t)\rangle = \sum_n C_n(\sqrt{N})|n\rangle \exp(-in\omega t), \tag{8}$$

where the C coefficients describe a Poisson distribution of the photon number around the average value N with dispersion $\langle(\Delta n)^2\rangle = N$.

The expectation values of the electric and magnetic fields on the ψ_{rf} state have the classical field expressions. The intensity of the rf field applied to the sample in a double-resonance experiment corresponds to a large number of photons, so that the relative dispersion $\sqrt{\langle(\Delta n)^2\rangle}/N = 1/\sqrt{N}$ is small. In the investigation of the time evolution of an atomic or molecular system the ψ_{rf} coherent state can be well represented through a state $|N\rangle$ with N rf photons.

For molecules with single-parity levels in the energy scheme of Fig. 1(b) the rf interaction is determined by the transition dipole matrix element between the $|2\rangle$ and $|3\rangle$ states. Introducing the operators σ and σ^+ defined by

$$\sigma|2\rangle = |3\rangle; \quad \sigma^+|3\rangle = |2\rangle \tag{9}$$

the rf field-molecule quantized interaction Hamiltonian in the dipole approximation takes the form[22]

$$V^{rf} = -\frac{E_r \mu_r}{2\sqrt{N}}(a + a^+)(\sigma + \sigma^+), \tag{10}$$

where the rotating wave approximation has been used, since $\mu_r E_r/\hbar \ll \omega$. The dressed molecule Hamiltonian is

$$H^d = H_m + H_{rf} + V^{rf} \tag{11}$$

and for $n \simeq N$ the eigenvectors and eigenvalues are

$$|+,N\rangle = \cos\theta\,|3\rangle|N-1\rangle + \sin\theta\,|2\rangle|N\rangle,$$
$$|-,N\rangle = -\sin\theta\,|3\rangle|N-1\rangle + \cos\theta\,|2\rangle|N\rangle, \quad (12)$$

and

$$E_{\pm} = \Omega_0 + N\omega \pm \omega_{\pm} = \Omega_0 + N\omega + \frac{\omega_0-\omega}{2} \pm \tfrac{1}{2}[(\omega_0-\omega) + (\mu_r E_r/\hbar)^2]^{1/2}, \quad (13)$$

where

$$\text{tg}\,2\theta = \frac{\mu_r E_r}{2\hbar(\omega_0-\omega)}, \quad 0 \leqslant \theta \leqslant \pi/2. \quad (14)$$

For molecules with double-parity levels the rf field interacts with the permanent dipole moment μ_1 or μ_2 in the $|1\rangle$ or $|2\rangle$ states of Fig. 1(a), and the interaction is described by the term

$$V^{\text{rf}} = -\frac{E_r}{2\sqrt{N}}(a+a^+)(\mu_1|1\rangle\langle 1| + \mu_2|2\rangle\langle 2|). \quad (15)$$

This interaction problem is formally equivalent to the problem of modulation of the static magnetic field in a magnetic resonance experiment, which has been already been solved by the dressed-atom approach.[23] In analogy to the results of Ref. 23, the dressed-molecule Hamiltonian H^d in the case of Fig. 1(a) has eigenstates

$$|\alpha,n\rangle = |\alpha\rangle|\bar{n}_\alpha\rangle = |\alpha\rangle\exp\left[(a^+ + a)\,\mu_\alpha E_r(\hbar 2\sqrt{N})^{-1}\right]|n\rangle \quad (\alpha = 1,2) \quad (16a)$$

and eigenvalues

$$E_{n\alpha} = \hbar\Omega_\alpha + n\hbar\omega - \mu_\alpha^2 E_r^2(\hbar 4N)^{-1}. \quad (16b)$$

The states $|1\rangle$ and $|2\rangle$ of the molecule are not mixed by the rf interaction, but the eigenstates of the dressed system involve rf states containing any number n of photons; for large n, as in the case of rf interaction, the matrix elements between the dressed system states satisfy the following relations[23]:

$$\langle\bar{n}_2|(\overline{n-q})_1\rangle = J_q[(\mu_1-\mu_2)E_r/\hbar\omega] = J_q(\zeta), \quad (17)$$

where $J_q(\zeta)$ is a q-order Bessel function of the ζ variable.

Let ρ^d, ρ^m, and ρ^{rf} denote the dressed system and the molecular and rf quantized field density matrices, respectively. ρ^m is obtained through a trace operation of ρ^d over the rf field variables. At the initial time, $t=0$, there is no correlation between the molecules and the rf field so that

$$\rho^d(t=0) = \rho^m(t=0) \otimes \rho^{\text{rf}}(t=0). \quad (18)$$

For a dilute molecular system and a very large number of the photons, the rf field-molecule correlations created by the interaction are very small.[24] Thus, it is a good approximation to describe the time evolution of the rf field density matrix as independent of the atomic interaction. Introducing the coherent state of Eq. (8), one finds

$$\rho^{\text{rf}}(t) = |\psi_{\text{rf}}(t)\rangle\langle\psi_{\text{rf}}(t)| = \sum_{nn'} C_n C_{n'}|n\rangle\langle n'|\exp[-i(n-n')\omega t]. \quad (19)$$

The molecular relaxation processes are assumed fast enough to be unaffected by the rf field, and the interference between the relaxation and the rf processes is assumed negligible. Within these assumptions, the time evolution equation of the ρ^d density matrix may be written

$$\left(\frac{\partial}{\partial t} + v\frac{\partial}{\partial z}\right)\rho^d = -\frac{i}{\hbar}[H,\rho^d] - \gamma\rho^d + \gamma\Lambda^m \otimes \rho^{\text{rf}} \quad (20)$$

with total Hamiltonian $H = H^d + V^{\text{IR}}$.

If we denote by $|a\rangle$ and $|b\rangle$ two eigenstates of the H^d dressed Hamiltonian, and by E_a and E_b their eigenvalues, the time evolution equation for the elements of the density matrix ρ^d gives

$$\left(\frac{\partial}{\partial t} + v\frac{\partial}{\partial z}\right)\langle a|\rho^d|b\rangle = -\left[\gamma + \frac{i}{\hbar}(E_a - E_b)\right]\times\langle a|\rho^d|b\rangle - \frac{i}{\hbar}\langle a|[V^{\text{IR}},\rho^d]|b\rangle + \gamma\sum_{n,n'}\langle a|1n\rangle\langle 1n'|b\rangle\Lambda^1 C_n C_{n'}^* \exp[-i(n-n')\omega t]. \quad (21)$$

Equation (21) has been obtained by introducing into the third term on the left-hand side of Eq. (20) the thermal equilibrium population in the $|1\rangle$ atomic state and the relation (19) for the $\rho^{\text{rf}}(t)$ density matrix. Once Eq. (21) has been solved, the molecular density matrix is derived from ρ^d by calculating the trace over the rf field states. For instance, for the three-level system of Fig. 1(b), if a state $|N\rangle$ with N photons is used to describe the rf state, the molecular coherence ρ_{21}^m is given by

$$\rho_{21}^m = \text{Tr}_{\text{rf}}\langle 2|\rho^d|1\rangle = \sin\theta\,\langle +,N|\rho^d|1,N\rangle + \cos\theta\,\langle -,N|\rho^d|1,N\rangle. \quad (22)$$

For levels with a permanent dipole moment, the eigenvectors $|\bar{n}_1\rangle$ of Eq. (16a) are a complete basis for the rf field manifold. Making use of Eq. (17) the molecular coherence ρ_{21}^m is given by

$$\rho_{21}^m = \sum_{n_1}\langle 2|\langle\bar{n}_1|\rho^d|\bar{n}_1\rangle|1\rangle = \sum_{n,p} J_{p-n}(\zeta)\langle 2,p|\rho^d|1,n\rangle. \quad (23)$$

III. INFRARED LASER RADIATION

To treat the IR–rf interaction, it is convenient to substitute in Eq. (21) the matrix elements of the IR field interaction of Eq. (2). For each configuration of Fig. 1 a separate solution has to be found.

A. Three-level system

The IR radiation interaction V^{IR} connects the levels $|1\rangle$ and $|2\rangle$ in the scheme of Fig. 1(a) and in the rotating wave approximation (RWA) has the following matrix elements between the dressed system eigenstates of Eq. (12):

$$\langle +,N|V^{\text{IR}}|1,N\rangle = -\sin\theta\mu_v E\exp(-i\Omega t)\cos kz/2,$$
$$\langle -,N|V^{\text{IR}}|1,N\rangle = -\cos\theta\mu_v E\exp(-i\Omega t)\cos kz/2. \quad (24)$$

As a consequence of the rf coupling between the $|2\rangle$ and $|3\rangle$ levels, the IR radiation induces transitions between the lower dressed state $|1,N\rangle$ and both the closely spaced upper dressed states $|+,N\rangle$ and $|-,N\rangle$. This three-level configuration with two transitions sharing a common level is well known in quantum optics[10,17] and several Doppler-free resonances, as dips, crossover saturation etc., are produced by the saturation of the IR field. In the dressed three-level system a single frequency IR field induces both the transitions.

The steady-state solution of the dressed density matrix equations may be written in Fourier expansions[17]:

$$\langle +,N|\rho^d(v,z,t)|-,N\rangle = (\exp -i(\omega_+ - \omega_-)t)\sum_{q,\text{even}} \sigma^q_{+,-}(v)\exp(+iqkz),$$

$$\langle \pm,N|\rho^d(v,z,t)|1,N\rangle = (\exp -i\Omega t)\sum_{q,\text{odd}} \sigma^q_{\pm,1}(v)\exp(+iqkz), \tag{25}$$

$$\langle \alpha,N|\rho^d(v,z,t)|\alpha,N\rangle = \sum_{q,\text{even}} \sigma^q_{\alpha,\alpha}(v)\exp(iqkz) \quad (\alpha = +,-,1).$$

By substituting Eqs. (25) in Eqs. (21) and isolating the Fourier components with the same spatial dependence, the following relations for the steady state matrix elements are obtained:

$$M^q\sigma^q_{1,1} = \Lambda^1 W(v)\delta_{q,0} + ix\sin\theta\sum_{\mu=\pm1}(\sigma^{q-\mu}_{+,1} - \sigma^{q+\mu}_{1,+}) + ix\cos\theta\sum_{\mu=\pm1}(\sigma^{q-\mu}_{-,1} - \sigma^{q+\mu}_{1,-}), \tag{26a}$$

$$M^q\sigma^q_{+,+} = -ix\sin\theta\sum_{\mu=\pm1}(\sigma^{q-\mu}_{+,1} - \sigma^{q+\mu}_{1,+}), \tag{26b}$$

$$M^q\sigma^q_{-,-} = -ix\cos\theta\sum_{\mu=\pm1}(\sigma^{q-\mu}_{-,1} - \sigma^{q+\mu}_{1,-}), \tag{26c}$$

$$L^q_{+,-}\sigma^q_{+,-} = ix\sum_{\mu=\pm1}(\sin\theta\sigma^{q+\mu}_{1,-} - \cos\theta\sigma^{q-\mu}_{+,1}), \tag{26d}$$

$$L^q_{+,1}\sigma^q_{+,1} = ix\sum_{\mu=\pm1}[\sin\theta(\sigma^{q+\mu}_{1,1} - \sigma^{q+\mu}_{+,+}) - \cos\theta\sigma^{q+\mu}_{+,-}], \tag{26e}$$

$$L^q_{-,1}\sigma^q_{-,1} = ix\sum_{\mu=\pm1}[\cos\theta(\sigma^{q+\mu}_{1,1} - \sigma^{q+\mu}_{-,-}) - \sin\theta\sigma^{q+\mu}_{-,+}], \tag{26f}$$

where

$$M^q = \gamma + iqkv,$$

$$L^q_{jl} = \gamma + i[(\Delta_l - \Delta_j) + qkv] \quad (j,l = +,-,1) \tag{27}$$

with

$$\Delta_\pm = \Omega_0 + \omega_\pm - \Omega; \quad \Delta_1 = 0, \quad x = \mu_v E/4\hbar.$$

In absence of the rf field the angle θ is zero and Eqs. (26) reduce to those of a two-level system interacting with a standing-wave laser radiation.

B. Two-level system

In this case the IR interaction Hamiltonian has nonvanishing matrix elements between the eigenstates $|1p\rangle$ and $|2q\rangle$:

$$\langle 2q|V^{\text{IR}}|1p\rangle = \langle 2|\langle\bar{q}_2|V^{\text{IR}}|\bar{p}_1\rangle|1\rangle = -\frac{\mu_v}{2}E\exp(-i\Omega t)J_{q-p}(\zeta)\cos kz, \tag{28}$$

where the RWA and Eq. (17) have been used. The rf states are mixed by the rf interaction and the IR field has nonvanishing matrix elements connecting all states of the dressed system. As a consequence an infinite number of Doppler-free saturated absorptions appear.

By using the matrix elements of Eq. (28) in Eq. (21) which describes the time evolution, the steady-state solution may be written as

$$\langle 1p|\rho^d|2q\rangle = \exp(-i\Omega t)\sum_{s,r}^{s,\text{odd}} \pi^{s,r}_{p,q}(v)\exp(iskz - ir\omega t), \tag{29}$$

$$\langle \alpha p|\rho^d|\alpha q\rangle = \sum_{s,r}^{s,\text{even}} \sigma^{\alpha,s,r}_{p,q}(v)\exp(iskz - ir\omega t) \quad (\alpha = 1,2).$$

With the hypothesis of initial population only in the lower $|1\rangle$ state we get the following recurrence relations:

$$N^s_{p-q-r}\sigma^{2,s,r}_{p,q} = ix\sum_{\mu=\pm1}\sum_l\{J_{p-l}(\zeta)\pi^{s+\mu,r}_{l,q} - J_{l-q}(\zeta)(\pi^{\mu-s,-r}_{l,p})^*\},$$

$$N^s_{p-q-r}\sigma^{1,s,r}_{p,q} = i\Lambda^1 W(v)C_p(\sqrt{N})C_q(\sqrt{N})\delta_{s,0}\delta_{r,p-q} - ix\sum_{\mu=\pm1}\sum_l\{J_{l-q}(\zeta)\pi^{s+\mu,r}_{p,l} - J_{p-l}(\zeta)(\pi^{\mu-s,-r}_{l,q})^*\}, \tag{30}$$

$$K^s_{p-q-r}\pi^{s,r}_{p,q} = ix\sum_{\mu=\pm1}\sum_l\{J_{l-q}(\zeta)\sigma^{1,s+\mu,r}_{p,l} - J_{p-l}(\zeta)\sigma^{2,s+\mu,r}_{l,q}\},$$

where

$$N^s_p = \gamma + i(p\omega + skv),$$

$$K^s_p = \gamma + i(\Omega - \Omega_0 + p\omega + skv),$$

and $(\,)^*$ denotes the complex conjugate. From these equations it is clear that, apart from the thermal population term, the relevant dependence upon the rf states occurs through the $p-q$ difference. The solution of these equations will be discussed in the following paragraphs.

IV. THIRD-ORDER PERTURBATIVE SOLUTION

The equation for the reduced density matrix σ can be solved in an iterative scheme treating the IR interaction as

the parameter of a series expansion. In the third-order solution the Doppler-free saturation resonances are obtained.

A. Three-level system

The iterative perturbation solution of Eqs. (26) following the treatment of Schlossberg and Javan[25] determines the Doppler-free resonance for the three-level system. The main difference in the dressed molecule approach is that the molecular susceptibility χ depends on both $\sigma_{-,1}$ and $\sigma_{+,1}$, since it results from combining Eqs. (6), (22), and (25). Thus, the resonances appearing in these coherences have to be considered simultaneously in deriving the monitored signal. The double-resonance signal also appears at the third-order perturbation, because it is based on the saturation and probe effects produced by the IR field.

The zero-order solution of Eqs. (26) is obtained by setting $x = 0$:

$$\sigma^0_{1,1}(v) = \Lambda^1 W(v), \tag{31}$$

and all other density matrix elements vanish. In first order the solution is

$$\sigma^{\pm 1}_{+,1} = ix \sin\theta \Lambda^1 W(v)[\gamma + i(\Omega_0 + \omega_+ - \Omega \pm kv)]^{-1},$$
$$\sigma^{\pm 1}_{-,1} = ix \cos\theta \Lambda^1 W(v)[\gamma + i(\Omega_0 + \omega_- - \Omega \pm kv)]^{-1}, \tag{32}$$

and all other elements vanish.

In order to understand more precisely the mathematics of the dressed system let us derive the first order molecular bulk susceptibility $\chi^{(1)}$. From Eqs. (6), (22), (25), and (32) one finds

$$\chi^{(1)} = \frac{2\mu_v}{E}\int dv\{\sin\theta(\sigma^1_{+,1} + \sigma^{-1}_{+,1}) + \cos\theta(\sigma^1_{-,1} + \sigma^{-1}_{-,1})\}$$
$$= \frac{i\mu_v^2}{\hbar}\Lambda^1 \int W(v)dv\left\{\frac{\sin^2\theta}{\gamma + i(\Omega_0 + \omega_+ - \Omega + kv)} + \frac{\cos^2\theta}{\gamma + i(\Omega_0 - \omega_- - \Omega + kv)}\right\}$$
$$= \mu_v^2 \Lambda^1 Z[\gamma + i(\Omega_0 - \Omega)]/\hbar, \tag{33}$$

where the plasma dispersion formula $Z(x + iy)$ has been introduced. In the plasma dispersion function we have set $\omega_- = \omega_+ = 0$ because in the typical rf double-resonance experiments the rf field is in resonance with the splitting ω_0 and the rf Rabi frequency $\mu_r E_r/\hbar$ is small compared to the Doppler width.

Equation (33) shows that the $\chi^{(1)}$IR susceptibility does not depend on the rf field.

Because the populations in the excited states $|2\rangle$ and $|3\rangle$ at the thermal equilibrium have been neglected, the double-resonance signal originates from the IR pumping of molecules from the ground level $|1\rangle$ to the level $|2\rangle$, and this pumping appears only in the second-order perturbation process. Introducing a thermal equilibrium population in the excited states $|2\rangle$ and $|3\rangle$, a first-order double-resonance signal appears, dependent on the thermal equilibrium population difference between the $|2\rangle$ and $|3\rangle$ states.

In the second-order perturbation the dressed populations and the rf coherence $\sigma^i_{+,-}$ $(i = 0,2,-2)$ are obtained. The third-order solution of Eqs. (26) gives the IR coherences $\sigma^{\pm 1}_{+1}$ and $\sigma^{\pm 1}_{-,1}$ which, once substituted in Eqs. (22) and (6), determine the third-order susceptibility $\chi^{(3)}$. For a Doppler-broadened IR line with $\gamma \ll ku$, several terms in the $\chi^{(3)}$ susceptibility vanish, and the remaining terms are produced by the processes schematically represented in Fig. 3.

The perturbative processes *a*, *b*, and *c* of Fig. 3 contribute to the double-resonance signal observed on the laser output at $\omega = \omega_0$ and involve saturation of the IR transition by one running wave and detection of the saturation by the same running wave. In Figs. 3(a) and 3(b) the IR saturation modifies the populations of the dressed-molecule eigenstates, while in Fig. 3(c) the rf coherences $\sigma_{+,-}$ and $\sigma_{-,+}$ appear in the second-order perturbation. The third-order susceptibility connected to the double-resonance processes is

$$\chi^{(3)}_{DR} = -2i\Lambda^1 \frac{\sqrt{\pi}}{ku}\frac{|x|^2}{\gamma}\frac{\mu_v^2}{\hbar}\left\{\frac{\cos^4\theta}{2\gamma} + \frac{\sin^4\theta}{2\gamma}\right.$$
$$\left. + \frac{\cos^2\theta\sin^2\theta}{2\gamma + i(\omega_+ - \omega_-)}\left[1 + \frac{\gamma}{2\gamma + i(\omega_+ - \omega_-)}\right] + \text{c.c.}\right\}$$
$$\times \exp[-(\Omega - \Omega_0)^2/(ku)^2]. \tag{34}$$

In the exponential evaluation a term ω_+ or ω_- has been neglected compared to $\Omega - \Omega_0$ because the double-resonance frequency region is investigated. The change in the third-order susceptibility produced by switching on–off the rf field is

$$\Delta\chi^{(3)}_{DR} = \chi^{(3)}_{DR}(\text{rf on}) - \chi^{(3)}_{DR}(\text{rf off})$$
$$= i\Lambda^1 \frac{\sqrt{\pi}}{ku}\left(\frac{\mu_v E}{2\hbar}\right)^2 \frac{\mu_v^2}{\hbar}\frac{(\mu_r E_r/\hbar)^2}{\gamma^2 + (\omega - \omega_0)^2 + (\mu_r E_r/\hbar)^2}$$
$$\times \exp[-(\Omega - \Omega_0)/(ku)^2]. \tag{35}$$

This double-resonance equation contains a Lorentzian line shape with a linewidth determined by the saturation broadening parameter $\mu_r E_r/\hbar$. The exponential term takes into account the fact that the signal is produced by those molecules which are Doppler shifted in resonance with the laser. The susceptibility of Eq. (34) is defined for a single laser running wave; for a laser intracavity standing wave two molecular groups with velocities $v = \pm(\Omega - \Omega_0)k^{-1}$ interact with the standing waves and give equal contributions to the double-resonance signal.[3] The third-order susceptibility of Eq. (35) has the same sign as the first-order susceptibility of Eq. (33), whence the double resonance produces an increase in the laser intracavity absorption and a decrease in the laser output power.

The inverted Lamb-dip susceptibility described by the

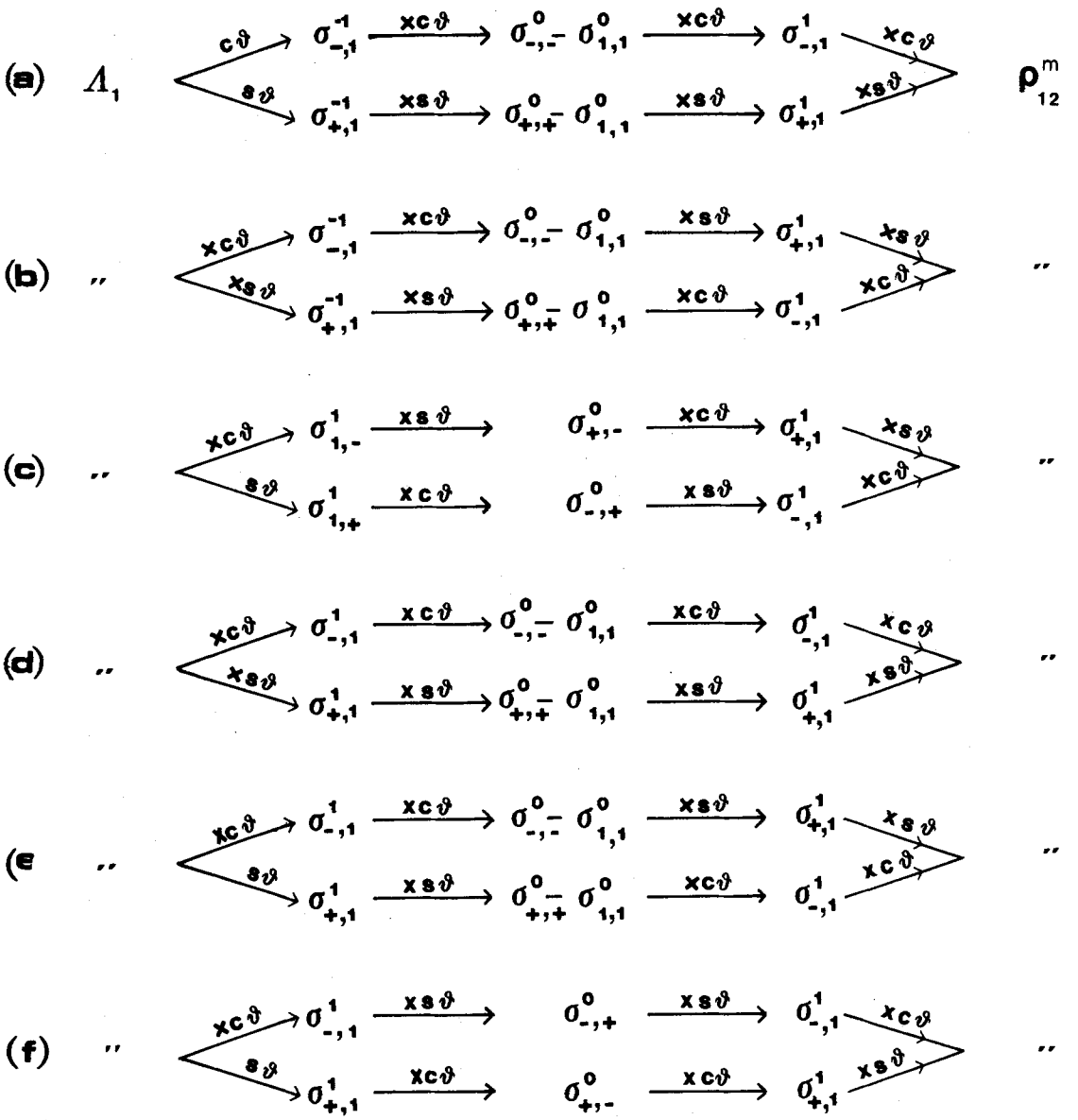

FIG. 3. Iteration processes in the third-order perturbation calculations of a three-level system. The processes (a), (b), (c) describe the double-resonance signal; the process (d) is the inverted Lamb dip; the process (e) is the crossover-saturation resonance; and the last process is a combination of Lamb-dip and Raman effect.

process of Fig. 3(d) is given by

$$\chi_{\mathrm{LD}}^{(3)} = -2i\Lambda^1 \frac{\sqrt{\pi}}{ku}\left(\frac{\mu_v E}{2\hbar}\right)^2 \frac{\mu_v^2}{\gamma\hbar} \times\left\{\frac{\cos^4\theta}{\gamma - i(\Omega - \Omega_0 - \omega_-)} + \frac{\sin^4\theta}{\gamma - i(\Omega - \Omega_0 - \omega_+)}\right\}. \tag{36}$$

Two inverted Lamb dips appear on the laser output at the laser frequencies $\Omega = \Omega_0 + \omega_\pm$. For a weak rf field the Lamb-dip positions become $\Omega = \Omega_0$ and $\Omega = \Omega_0 + \omega_0 - \omega$, respectively, i.e., the Lamb dip on the 1–2 transition of Fig. 1(b) and the two-photon IR–rf Lamb dip on the 1–3 transition. The rf field intensity shifts the position of the Lamb dip following the dressed molecule eigenenergies ω_+ and ω_-. The dependence of the Lamb-dip intensities on the rf amplitude is given by the $\cos^4\theta$ and $\sin^4\theta$ factors in Eq. (36). In the paper by Freund and Oka[9] on the two-photon IR–rf Lamb dips the rf field interaction was treated as a perturbation and only the lowest order terms in the rf field amplitude series expansion of Eq. (36) were obtained.

The dressed-molecule crossover resonance, represented by the perturbative path of Fig. 3(e), is typical of a three-level system irradiated by two lasers. The saturation of a transition by an IR running wave is probed by another IR running wave on a transition sharing a common level with the first one. In the scheme of the undressed molecule the crossover saturation is originated by the simultaneous presence of the one-photon IR transition and the two-photon IR–rf transition. The third-order susceptibility for this process is

$$\chi_{\mathrm{CS}}^{(3)} = -2i\Lambda^1 \frac{\sqrt{\pi}}{ku}\left(\frac{\mu_v E}{2\hbar}\right)^2 \frac{\mu_v^2}{\gamma\hbar}$$

$$\times \frac{\sin^2\theta\cos^2\theta}{\gamma - i[\Omega - \Omega_0 + (\omega - \omega_0)/2]} \times \exp[-(\omega_+ - \omega_-)^2/(2ku)^2]. \quad (37)$$

$\chi_{CS}^{(3)}$ describes a Doppler-free saturation signal occurring at $\Omega = \Omega_0 + (\omega_0 - \omega)/2$ for molecules having a velocity $v \simeq \pm c(\omega_0 - \omega)/(2\Omega)^{-1}$ along the z axis. This Doppler-free resonance, that may be regarded as a velocity tuned IR–rf Lamb dip was not considered by Freund and Oka.[9] However, it was later observed in experiments involving transitions in the microwave[6] and radio frequency range.[10,16,26]

The third-order susceptibility of the process of Fig. 3(f) contains terms describing the time evolution of these rf coherences:

$$\chi_{IR}^{(3)} = -i\Lambda^1 \frac{\sqrt{\pi}}{ku}\left(\frac{\mu_v E}{2\hbar}\right)^2 \frac{\mu_v^2}{\hbar}\left\{\frac{1}{\gamma - i(\omega_+ - \omega_-)}\cdot\frac{1}{\gamma - i(\Omega - \Omega_0 - \omega_-)}\exp[-(\Omega - \Omega_0 - \omega_-)^2(k\mu)^{-2}]\right.$$

$$\left. + \frac{1}{\gamma + i(\omega_+ - \omega_-)}\cdot\frac{1}{\gamma - i(\Omega - \Omega_0 - \omega_+)}\exp[-(\Omega - \Omega_0 - \omega_+)^2(ku)^{-2}]\right\}. \quad (38)$$

As pointed out by Schlossberg and Javan,[25] Eq. (38) describes a combination of Lamb-dip Raman effects. The Raman-like $[\gamma \pm i(\omega_+ - \omega_-)]^{-1}$ dependence, is produced by a single laser running wave acting on both the $- \leftrightarrow 1$ and $+ \leftrightarrow 1$ transitions. The Lamb-dip effect, with the $[\gamma - i(\Omega - \Omega_0 - \omega_\pm)]^{-1}$ dependences, arises from different running waves acting on the same transition. A phase matching condition results from the derivation of $\chi_{LR}^{(3)}$ but in the dressed-molecule case this condition is automatically satisfied because a single IR field produces the phenomenon through the single- and two-photon transitions. Our numerical analysis shows that the $\chi_{LR}^{(3)}$ signal usually has a negligible contribution as compared to the Lamb-dip and crossover signals. A comparison of Eqs. (36) and (37) for the Doppler-free saturation signals with the double-resonance expression of Eq. (35) shows that the susceptibility in the Doppler-free resonances has both real and imaginary contributions, while the double-resonance susceptibility only has an imaginary term. Thus, the saturated absorption signals produce changes in laser frequency and laser power, while the double resonance modifies the laser power only. A comparison of the imaginary parts of Eqs. (36) and (37) to the susceptibility of Eq. (33) shows that the inverted Lamb dip and the crossover resonance produce an increase in the laser output power.

In the intracavity experiments the IR–rf signal may be observed in two different arrangements: at a fixed laser frequency the rf field frequency is swept over the resonance value or the rf field is fixed in frequency and amplitude and the laser frequency is swept over its tuning profile. Both cases have been experimentally investigated and radio frequency splittings plus infrared transitions have been determined through those measurements. By sweeping the rf field frequency, typical in the double-resonance experiments, the observed power depends upon the rf frequency ω through the sum of the double-resonance signal of Eq. (34) and the saturation signals of Eqs. (36)–(38). The double-resonance contribution of Eq. (34) has a Lorentzian line shape, but this line shape is modified by the contribution of the Doppler-free resonances. This modification has been investigated in a previous paper.[18]

We will analyze here the experiments where the frequency and the intensity of the rf field are fixed and the laser frequency is swept, as is done, for instance, in Ref. 10. As discussed in the Introduction, the line shape of the signals observed on the laser output power is determined by the laser frequency dependence of the absorption coefficient χ'', i.e., the imaginary part of the molecular susceptibility. In the absence of an rf field, the molecular absorption coefficient presents the inverted Lamb-dip signal at $\Omega = \Omega_0$, i.e., an increase in the laser output power when the laser frequency is in resonance with the IR absorber frequency. The application of the rf field produces a splitting of the IR Lamb dip into two separate IR–rf Lamb dips, represented by the two terms of Eq. (36), with an intensity proportional to $\cos^4\theta$ and $\sin^4\theta$, respectively. Moreover, the rf field produces the new Doppler-free signals of the crossover saturation [Eq. (37)] and the Raman–Lamb dip [Eq. (38)]. In the experiment of Ref. 10 the rf field amplitude was modulated on–off and a phase sensitive detection was used. Thus the quantity $\Delta\chi'' = \chi''(\text{rf on}) - \chi''(\text{rf off})$ has to be compared to the signals observed on the laser output power. Figure 4 is a plot of this quantity vs the laser frequency detuning expressed in reduced units: $dl = (\Omega - \Omega_0)/\gamma$. A positive $\Delta\chi''$ leads to a decrease in the laser output power; a negative $\Delta\chi''$ to an increase in the laser power. The reported line shapes may be compared to the signals recorded in Ref. 10. Different line shapes are observed by varying the two rf parameters, i.e., the detuning $d = (\omega - \omega_0)/\gamma$ normalized to the relaxation rate and the normalized Rabi frequency $r = \mu_r E_r/\hbar\gamma$. When the rf field is in resonance ($d = 0$), the IR–rf Lamb dips, have an equal intensity and occur at $\Omega = \Omega_0 \pm \gamma r/2$. Figures 4(a) and 4(b) present this phenomenon, called coherence splitting, for different values of the Rabi frequency, $r = 2$ and 10, respectively. In the $\Delta\chi''$ difference plot of Fig. 4(b) the two upwards peaks correspond to the IR–rf Lamb dips, while the downwards peak is the unperturbed inverted IR Lamb dip. In Fig. 4(a), at a lower r value, the frequency separation of the two IR–rf Lamb dips from the central IR Lamb dip is small, and the different peaks are not resolved. Figs. 4(c)–4(f) present the Doppler-free resonance in the presence of a detuned rf field. By inverting the sign of d, the

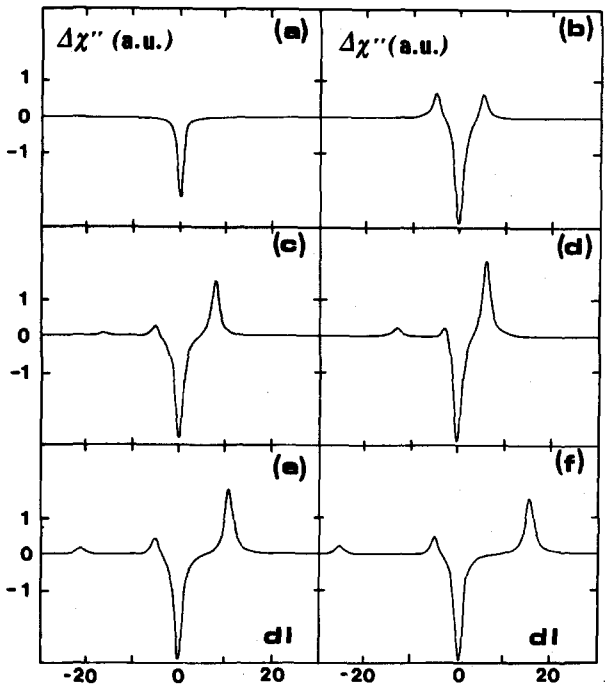

FIG. 4. The change $\Delta\chi''$ in the imaginary part of the susceptibility vs the laser frequency detuning dl, as obtained from the third-order dressed-molecule approach for different values of the rf parameter: curve (a) $d=0$, $r=2$; curve (b) $d=0$, $r=10$; curve (c) $d=5$, $r=20$; curve (d) $d=10$, $r=20$; curve (e) $d=10$, $r=30$; curve (f) $d=10$, $r=40$.

rf detuning, the curve of $\Delta\chi''$ vs dl is changed to the mirror image with respect to the vertical $\Omega=\Omega_0$ axis. Figures 4(c) and 4(d) have been obtained at a fixed Rabi frequency $r=20$, and different detunings 5 and 10, respectively. In Figs. 4(c)–4(f) the detuning is fixed at $d=10$ and r is equal to 30 and 40, respectively. Owing to the choice of the rf parameter, all the IR–rf peaks are well separated from the central inverted IR Lamb dip. The central peak, at $\Omega=\Omega_0-d\gamma/2$, corresponds to the crossover saturation. The two external peaks, at the position $\Omega=\Omega_0\pm\omega_\pm$, are the IR–rf Lamb dips. In the scheme of the undressed molecule the weaker Lamb dip, at lower Ω frequencies, is interpreted as the two-photon IR–rf Lamb dip on the 1–3 transition of Fig. 1(b). Increasing the rf intensity parameter r, the amplitude of the IR–rf Lamb dips increase, and their distance from the central IR Lamb dip at $\Omega=\Omega_0$ is increased. In the experimental investigation of the rf–IR Doppler-free resonance it is convenient to increase the intensity of the rf field because larger signals are obtained. However, great care should be taken in using the IR–rf Lamb dips for the measurements of the molecular transitions because their position is strongly affected by the rf field intensity. On the contrary, as it appears from the curves of Figs. 4(c)–4(f), the crossover resonance appears at the position $\Omega=\Omega_0+(\omega_0-\omega)/2$, which is unaffected by the r parameter. Thus, accurate precision transition measurements may be performed making use of the crossover resonances.

B. Two-level system

The perturbation solution for the set of Eqs. (30) describing the time evolution of the density matrix σ starts from the zeroth order solution:

$$\sigma_{p,q}^{1,0,p-q}=\Lambda^1 W(v)C_p(\sqrt{N})C_q^*(\sqrt{N}) \tag{39}$$

while all other density matrix elements vanish. The first-order susceptibility is obtained from the first-order infrared coherences making use of Eqs. (6) and (23):

$$\chi^{(1)}=\mu_v^2\Lambda^1\sum_n J_n^2(\zeta)Z[\gamma+i(\Omega_0+n\omega-\Omega)]/\hbar. \tag{40}$$

The index n, describing the number of rf photons involved in the multiphoton IR–rf absorption, is much smaller than the variance N of the Poisson distribution of Eq. (8). Thus we have made the approximation $C_{n+q}\simeq C_q$. The $\chi^{(1)}$ expression represents how an absorption line splits into sidebands at frequencies $n\omega$. The nth sideband, arising from a multiphoton process involving n rf photons, has an intensity determined by the nth Bessel function. Similar expressions for the susceptibility are obtained in the modulation experiments of molecular spectroscopy and magnetic resonance.

The third-order susceptibility is derived through the perturbative calculation of the populations and infrared coherences. Making use of the residue theorem for the velocity integration,[2] the third-order susceptibility results:

$$\chi^{(3)}=-2\pi i\frac{\mu_v^2}{\hbar}x^2\sum_{p,q,r}W\left(\frac{2p-r}{2}\omega\right)\times\frac{J_p(\zeta)J_{p+q}(\zeta)J_{p-q+r}(\zeta)J_{r-p}(\zeta)}{[\gamma+iq\omega][2\gamma-i2(\Omega-\Omega_0)-ir\omega]}. \tag{41}$$

The numerator of this expression contains the IR–rf interaction elements involved in the perturbative treatment. The velocity function W selects the molecules involved in the Doppler-free resonances. The $[\gamma+iq\omega]$ dependence in the denominator arises from the rf coherence appearing in the second-order perturbation.

The Doppler-free resonances described by Eq. (41) have contributions from Lamb-dip and crossover resonances. Because the IR–rf interaction connects all the dressed molecule levels, an infinite number of Doppler-free resonances arise with an intensity dependent on the parameter $\zeta=(\mu_1-\mu_2)E_r/\hbar\omega$ of the Bessel function. Our formal derivation of the two-level third-order susceptibility justifies the expressions of Refs. 2, 10, and 11, where a comparison with the experimental results on the sidebands was presented.

Here we use Eq. (41) to interpret another important feature observed in the rf intracavity experiments, the so-called zero-field signal[3,16]: when the rf field is frequency swept around $\omega\simeq 0$, the laser output power shows a large decrease in intensity. At low frequencies the sideband components of Eq. (41) are not resolved and $\chi^{(3)}$ is the unstructured composition of the sideband absorptions. Increasing ω, the imaginary part of the third-order susceptibility decreases in intensity, and a signal with half-width determined by γ is represented by that equation. The strength of this signal depends on the modulation parameter ζ because higher order multiphoton components may give an important contribution in the summation. A large $\chi^{(3)}$ susceptibility is originated only when $\Omega\simeq\Omega_0$, and the appearance of the zero-field signal is direct evidence for the laser frequency

being in near resonance with an infrared transition of the absorber. In effect, the zero-field signal was used to search for the coincidence of the laser lines with absorber transitions.[3] Our analysis shows that the zero-field signal depends on the difference between the permanent molecular dipole moments in the lower and upper IR states.

V. CONTINUED FRACTION IN THE THREE-LEVEL SYSTEM

In the presence of a strong IR field, the higher order terms in the iteration expansion of the density matrix are required to describe the experimental results. For instance the fifth-order perturbation in the dressed molecule is required to interpret the velocity-tuned IR–rf multiphoton Lamb dips observed by Freund *et al.*[11] in the two-level system and by Jones[6] in the three-level system. The saturation phenomena of those transitions are described by terms involving higher order perturbations. An alternative approach valid for any IR field intensity is based on the continued fraction solution: the density matrix elements are formally expressed through a continued fraction involving an infinite number of terms. For laser standing-wave configurations a solution based on matrix continued fractions was introduced in Ref. 27.

For two-level molecules with a permanent dipole moment, Eqs. (30) have to be solved. They are formally equivalent to those of a system with an infinite number of equispaced levels interacting with a standing wave radiation. The density matrix elements of such a system may be formally expressed through a solution involving continued fraction of infinite order matrices, as sketched out in Ref. 28. The numerical evaluation of these matrix fractions presents a high degree of complexity.

The continued fraction solution for a three-level dressed molecule interacting with an IR standing-wave laser is obtained from the mathematical analysis developed in Ref. 17. In Eqs. (26) we may eliminate the optical coherences making use of Eqs. (26e) and (26f) where they are defined as function of the population and the rf coherences. Thus we get a set of recurrence relations involving $\sigma^q_{1,1}-\sigma^q_{+,+}$, $\sigma^q_{1,1}-\sigma^q_{-,-}$, $\sigma^q_{+,-}$, and $\sigma^q_{-,+}$ only. These recurrence relations may be written as

$$W^{-1}_q X^{q-2} + W^0_q X^q + W^{+1}_q X^{q+2} = J^0 \delta_{q,0}, \tag{42}$$

where the four-component vectors X^q and J^0 are defined by

$$X^q \equiv (\sigma^q_{1,1}-\sigma^q_{+,+}, \sigma^q_{1,1}-\sigma^q_{-,-}, \sigma^q_{+,-}, \sigma^q_{-,+}), \tag{43}$$

$$J^0 \equiv (\Lambda^1 \cos\theta, \Lambda^1 \sin\theta, 0, 0).$$

The elements of the 4×4 matrices $W(i=\pm1,0)$ are defined by the functions of Eqs. (27) in the Appendix of Ref. 17 when the following identifications are introduced:

$$\alpha^+ = \alpha^- = x\sin\theta,$$
$$\beta^+ = \beta^- = x\cos\theta, \tag{44}$$
$$M^q_j = \gamma + iqkr \quad \forall J.$$

The system of Eqs. (43) may be formally written in a form very convenient for numerical computation purposes:

$$X^0 = (W^{-1}_0 Z^{-1}_{-2} + W^0_0 + W^1_0 Z^1_2) J^0, \tag{45a}$$
$$X^q = Z^{\pm1}_q X^{q\pm2} \tag{45b}$$

with the 4×4 matrices $Z^\mu_q(\mu=\pm1)$ given by

$$Z^\mu_q = -(W^0_q + W^\mu_q Z^\mu_{q+2\mu})^{-1} W^{-\mu}_q. \tag{45c}$$

The continued fractions of Eqs. (45) are evaluated numerically by truncation to a finite number of terms in the denominator. It is a standard procedure in the calculation to check if the addition of one term in the denominator modifies the numerical value within the required accuracy. From the solution of Eqs. (45), making use of Eqs. (26e) and (26f) the IR molecular susceptibility may be derived.

We have used the continued fraction solution to investigate the influence of the laser intensity on the line shape of the Doppler-free resonances. The absorption coefficient χ'' has been numerically evaluated for rf parameters similar to those of Fig. 4, while the IR Rabi frequency was varied. The curves of Fig. 5 represent the molecular absorption coefficient vs the laser frequency detuning when the rf field is resonant with the $|2\rangle$–$|3\rangle$ transition ($d=0$) at a fixed rf field intensity ($r=10$). Also the laser intensity has been expressed in reduced units as a function of the relaxation rate γ, $rl=\mu_v E/4\hbar\gamma$. In the different curves the laser intensity is progressively increased from $rl=5$, a low value not producing saturation of the IR transition, to $rl=5$, a large value corresponding to a strong saturation. At the low rl value the coherence splitting of the Lamb dip is obtained, equivalent to that reported in Figs. 3(a) and 3(b), and two rf–IR Lamb dips are located at $\Omega-\Omega_0=\pm\mu_r E_r/2\hbar$. Moreover, curve (a) of Fig. 5 presents a strong crossover resonance located at $\Omega=\Omega_0$.

This crossover resonance does not appear in Figs. 4(a) or 4(b) where the variation $\Delta\chi''$ produced by the rf field has been plotted. Such a crossover signal at the center of the coherence splitting was never observed in the experiments because either the rf field strength was not large enough to separate the IR–rf Lamb dips or the variation of $\Delta\chi''$ only was monitored. As shown in Figs. 5(b) and 5(c), increasing the IR laser intensity causes the Doppler-free resonances of Fig. 5(a) to be broadened and smeared out. In effect, in the experimental arrangement of the rf–IR multiphoton resonances, the laser operates just above threshold at moderate IR power. The vertical scales of the curves in Fig. 5 are in the same arbitrary units, and the susceptibility at a different laser power may be quantitatively compared. A decrease in the susceptibility produced by the saturation appears, but the absorbed laser power, proportional to χ'' times the square of the electric field intensity, increases with the laser power.

VI. CONCLUSIONS

In this paper we have demonstrated that the dressed-molecule approach is a very convenient method to interpret the experiments where rf and IR electromagnetic fields are simultaneously applied to a molecular system. The density matrix equations of the dressed molecule have been derived for two cases, the three-level and two-level systems, where the rf field is coupled, respectively, to the transition dipole moment or to the permanent molecular dipole moment.

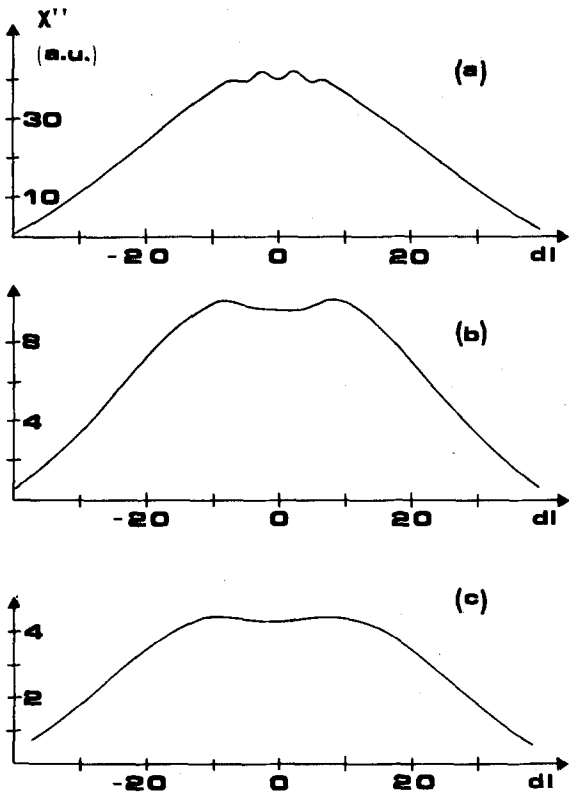

FIG. 5. Line shapes of the imaginary part of the susceptibility χ'' vs the laser frequency detuning dl, at $d = 0$ and $r = 10$, for different values of the laser intensity; $rl = 0.5, 2.5, 5$ in curves (a), (b), and (c), respectively.

When the transition and permanent dipole moments are simultaneously different from zero, the rf field is coupled to both, and the interaction Hamiltonian contains a larger number of terms. We have not exploited this case because of the complexity of the density matrix equations. Intracavity rf–IR experiments have dealt with configurations where the permanent and transition dipole moments are simultaneously interacting with the rf field. For instance, the zero-field signal arises from the permanent dipole moment of the double-parity levels, and the double-resonance signals are produced by the transition dipole moment of the three-level system. The spectra of Ref. 3, where the double-resonance transitions of the nuclear quadrupole structure have been observed, presents both double-resonance and zero-field signals for a three-level system with double-parity levels. Equations (35) and (41) may be used to analyze separately the zero-field and double-resonance signals by supposing that no interference exists between the two-level and three-level phenomena. Deformations in the line shape produced by such an interference have not been observed in the experiments. At the present time there are not experiments which would justify the mathematical and numerical efforts required to solve the most general case for the rf interactions.

The field amplitude perturbative solution of the density matrix equations provides a simple physical interpretation of the resonances produced by the laser field. The lowest order solution of the three-level case has been presented in Sec. IV A. In Sec. V the continued fraction solution involving 4×4 matrices has been applied to treat exactly the IR interaction in the three-level case. We have applied the continued fraction solution to very large laser field amplitudes for which the third-order approximation is no longer valid. At very large laser amplitudes, in the so called strong field regime, other nonlinear phenomena such as the velocity-tuned Lamb dips are produced.[20] These higher order Lamb dips cannot be observed directly on the laser output power when the laser frequency is scanned. Thus, the line shapes observed on the laser output power as derived in the continued-fraction treatment, do not show any new Doppler-free features in comparison to those derived with the third-order approximation. On the contrary, the intensity of the signals associated with the double resonance, the IR–rf Lamb dips, and the crossover resonance, appear greatly modified by the increase in the laser intensity. These phenomena are conveniently analyzed within the dressed-molecule description with a continued fraction solution.

Intracavity double-resonance and Lamb-dip experiments have been widely performed for accurate molecular spectroscopy measurements. In most experiments very low rf and IR powers were applied so that the signal distortion from a simple absorption line shape could be neglected. However, when distorted line shapes were observed, a quantitative analysis was not worked out, probably because an appropriate theoretical description was not available. The dressed-molecule model presented in this work provides such a description, as proved by the line shapes of Figs. 4 and 5 which correspond to the signals observed in some of the experiments of Refs. 2–10.

ACKNOWLEDGMENTS

Fruitful discussions with Takeshi Oka at the Herzberg Institute of Astrophysics of the National Research Council, Ottawa (Canada) where this work was started, are greatly acknowledged. The authors wish to thank R. Bernheim for a critical reading of the manuscript.

[1] K. Shimoda, in *Laser Spectroscopy of Atoms and Molecules*, Vol. 2 in Topics in Applied Physics, edited by H. Walther (Springer, New York, 1976), p. 84.
[2] T. Oka, in *Frontiers in Laser Spectroscopy*, Vol. 2 in Les Houches Summer School Proceedings Session XXVII, edited by R. Balian, S. Haroche, and S. Liberman (North-Holland, Amsterdam, 1977), p. 529; Philos. Trans. R. Soc. London Ser A **307**, 591 (1982).
[3] E. Arimondo, P. Glorieux, and T. Oka, Phys. Rev. A **17**, 1375 (1978).
[4] W. A. Kreiner and T. Oka, Can. J. Phys. **53**, 2000 (1975).
[5] E. Arimondo, P. Glorieux, and T. Oka, in *Laser Spectroscopy III*, edited by J. L. Hall and J. L. Carlsten (Springer, New York, 1977), p. 287.
[6] H. Jones, J. Mol. Spectrosc. **70**, 279 (1978).
[7] M. Allegrini, A. R. W. McKellar, P. Pinson, and J. M. Brown, J. Chem. Phys. **73**, 6086 (1980).
[8] B. Macke, P. Glorieux, A. Jacques, and J. Legrand, J. Phys. B **14**, 447 (1981).
[9] S. M. Freund and T. Oka, Appl. Phys. Lett. **21**, 60 (1972); Phys. Rev. A **13**, 2178 (1976).
[10] E. Arimondo and P. Glorieux, Phys. Rev. A **19**, 1067 (1979).
[11] S. M. Freund, M. Romheld, and T. Oka, Phys. Rev. Lett. **35**, 1497 (1975).

[12]R. G. Brewer and E. L. Hahn, Phys. Rev. A **11**, 1641 (1975).
[13]R. F. Wormsbecher, D. O. Harris, and B. G. Wicke, J. Mol. Spectrosc. **64**, 86 (1977).
[14]M. Takami, Jpn. J. Appl. Phys. **15**, 1063, 1889 (1976).
[15]F. Shimizu, Phys. Rev. A **10**, 950 (1974).
[16]A. Jacques and P. Glorieux, in *Laser Spectroscopy V*, edited by A. R. W. McKellar, T. Oka, and B. Stoicheff (Springer, New York, 1981), p. 140; Appl. Phys. B **26**, 217 (1981); Opt. Commun. **40**, 201 (1982).
[17]R. Vilaseca, G. Orriols, L. Roso, R. Corbalan, and E. Arimondo, Appl. Phys. B **34**, 73 (1984).
[18]A. Sasso and E. Arimondo, Lett. Nuovo Cimento **37**, 417 (1983).
[19]E. Arimondo and T. Oka, Phys. Rev. A **26**, 1494 (1982).
[20]B. J. Feldman and M. S. Feld, Phys. Rev. A **1**, 1375 (1970).
[21]M. Sargent III, M. O. Scully, and W. E. Lamb, Jr., *Laser Physics* (Addison–Wesley, Reading, Mass., 1974).
[22]C. Cohen-Tannoudji, *Cargese Lectures in Physics*, edited by M. Levy (Gordon and Breach, London, 1968), Vol. 2, p. 347.
[23]N. Polonsky and C. Cohen-Tannoudji, J. Phys. (Paris) **26**, 409 (1965).
[24]S. Haroche, Ann. Phys. (Paris) **6**, 189, 327 (1971).
[25]H. R. Schlossberg and A. Javan, Phys. Rev. **150**, 267 (1966).
[26]P. Glorieux and G.W. Hills, J. Mol. Spectrosc. **70**, 459 (1978).
[27]A. Bambini, Phys. Rev. A **14**, 1479 (1976); M. Allegrini, E. Arimondo, and A. Bambini, *ibid.* **15**, 718 (1977).
[28]A. Bambini and M. A. Zoppi, Phys. Lett. **59** A, 379 (1976).